# New Horizons of Visualization
## Anatomically Correct Rendering of Target Volumes Based on 3D-CISS Data Records

K. E. W. Eberhardt[1,2], C. Rezk-Salama[3,4], B. Tomandl[2], M. Deimling[3], A. Scola[1], R. Schindler[5], M. Dütsch[6], F. A. Fellner[7,8]

[1]*Institute of Diagnostic and Interventional Radiology, Municipal Hospital of Schweinfurt, Schweinfurt, Germany*
[2]*Division of Neuroradiology, Department of Neurosurgery, Erlangen-Nuremberg University, Erlangen, Germany*
[3]*Siemens AG, Medical Solutions, Erlangen, Germany*
[4]*Institute for Graphic Data Processing, Erlangen-Nuremberg University, Erlangen, Germany*
[5]*Inside, Functional Diagnostic Inc., Schweinfurt, Germany*
[6]*Department of Neurology, Erlangen-Nuremberg University, Erlangen, Germany*
[7]*Institute of Radiology, Upper Austrian State Hospital Wagner-Jauregg, Linz, Austria*
[8]*Institute of Diagnostic Radiology, Erlangen-Nürnberg Friedrich-Alexander University, Erlangen, Germany*

## Keywords

• CISS • VRT • anatomy • segmentation

## Introduction

The high radiation absorption rate of calciferous structures (bones) or structures after contrast enhancement (vessels) makes it possible to (implicitly) segment data records from CT examinations using robust and simple threshold-based algorithms. As opposed to CT, data cannot be segmented using simple threshold values with MRI despite the far better soft-tissue resolution, due to the high dispersion of signal intensity in the individual measurement volumes (voxels). A comparatively complex sorting of data (explicit segmentation) is generally required before actual rendering can take place. It is therefore not surprising that post-processing has in the past been modeled after the capabilities offered by threshold-based CT methods. In contrast to previous rendering procedures, which are based on algorithms that acquire the structure of surfaces using different virtual lighting perspectives (SSD) or the density or intensity profile along an imaginary central beam (MIP), i.e., only draw upon a few, selected voxels for reconstruction, more recent techniques use all voxels, i.e., the entire volume (VRT) for imaging purposes. There are two advantages to viewing whole volumes:

1. As opposed to SSD and MIP, partial volumes can be created, color-coded and saved. The partial volumes can be added to or subtracted from other partial volumes as desired, which enables an anatomically correct imaging without disruptive overlays. Up to four partial volumes can be obtained from a single data record and allocated to specific structures in this way.

2. The volumes determined in this way can be quantified, which enables a standardized, precise progress check and evaluation of therapeutic effects.

To simplify the complex sorting of data, however, the dispersion of signal intensity must be reduced. The most effective way to achieve this is by using modified MR sequences. The following paper describes the segmentation and visualization results of an examination sequence specifically modified to meet the requirements of optimized post-processing, and presents examples for initial practical applications for the clinical routine.

## Material and Methods

### 3D-CISS

Selected anatomical structures can be imaged in a targeted manner through the careful selection of parameters in MR sequences. Differentiating vascular structures from the surrounding subarachnoid space requires the use of strongly $T_2$-weighted sequences, in which the vascular structures appear as signal-free structures, i.e., as voids in the bright surrounding CSF. Neuronal structures also appear low-signal, and well delineated from the subarachnoid space. As a third tissue component, fatty tissue exhibits a signal that is elevated, even though reduced relative to CSF. The CISS sequence represents a sequence that sufficiently satisfies this requirement profile [1]. The examinations below were performed using this sequence. Fig. 1 shows that the space between the spinal cord and pachymeninx (dura) is filled with CSF, and envelops the targeted spinal vascular structures. The dura itself is enveloped by structures with little or no signal intensity (bones) and signal-rich fatty tissue, which is adjacent to the latter from outside (epidural). The spinal cord itself has a low-signal. The signal relationships in the spinal canal are comparable to those in the brain: Gray and white brain matter (as well as cranial nerves) have a low signal, vessels are signal-
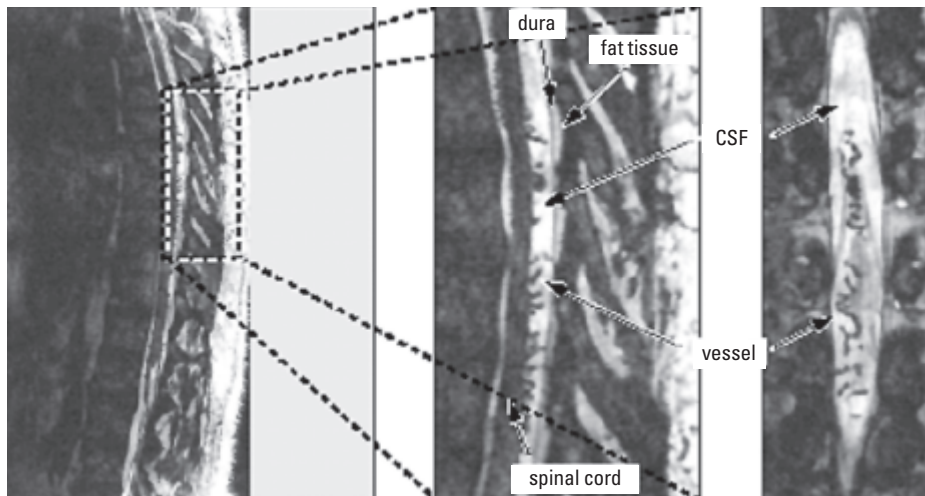
Fig. 1
Secondary multiplanar
2D-reconstruction of a 3D-CISS
data record.

MR-CISS data record of a dAV in
the area of the thoracic spine:

(*left*): Sagittal sectional view,
unmagnified;

(*middle*): Magnified sagittal
views show the target volumes
(vessels and CSF);

(*right*): Magnified multi-planar
coronary 2D image reconstruction.

free because of motion of the spins during the measurement interval, and CSF is bright. Because nerve tissue, vessels and bones have similar signal values, it is impossible to render these structures using a simple algorithm like MIP, since this would result in disruptively overlapping images. However, explicitly segmenting such thin vascular and neural structures is a difficult process fraught with errors, given the low resolution of these structures and the high partial volume effect, i.e., the probability that tissue of varying signal intensity will be measured within the same voxel. Direct interactive volume rendering offers one solution, as it permits semi-transparent representations, and also makes it possible to differentiate exact vascular structures from surrounding structures [2].

This requires that individual color coding tables be used for the subarachnoid space. One prerequisite for this purpose is that it be possible to interactively use the transfer functions with which the MR signal value is converted into an "image value". Proceeding in this way ensures an implicit, i.e., threshold-based segmentation of even complex MRI data in a very short time.

### Visualization

Direct volume rendering is superior to other approaches based on polygonal elements [3, 4] when it comes to the spatially allocated rendering of tomographic data [5, 6]. The option of having the segment volumes from the respective operation available interactively at any time for visual feedback as an image with a sufficiently high resolution is an important precondition for clinical application [7, 8]. As shown [9], 3D texture mapping enables the required hardware-accelerated trilinear interpolation of data.

Thus, a 3D image of the volume is generated by establishing a sufficient number of equidistant, semi-transparent polygons parallel to the image plane, taking into account the current image plane. While a lattice is created in this way, the image information of the expected polygons is taken directly from the 3D texture of the trilinear interpolation. In this way, the resultant image is generated by superposing the "described" polygons into the image plane from the back forward. The transfer function is allocated to the 3D texture in the lattice (grid), so that the color and opacity can be determined from the original data record for each individual voxel.

Using special computer hardware allows us to interactively modify the image tables, which enables direct visual feedback. In this way, the semi-transparent mode of viewing leads to a rapid and controlled implicit segmentation of image data. As a result, exact vascular structures and complex target structures can be displayed and differentiated in a highly effective manner. In addition, this is the best way to minimize partial volume effects and inherent noise which pose major problems with an explicit approach [10].

Since each individual voxel receives a specific marker (*"Tag"*) during voxel-based segmentation, an allocation to specific sub-units is possible. The global image table is divided into individual areas based on the varying tags. This makes individual transfer functions for color and opacity values available for each sub-volume, which in the end enables a targeted correction of the local 3D data.

### Segmentation

As already explained, CISS data records exhibit a very large signal difference between CSF and all other surrounding structures, with the exception of fatty epidural tissue. Vascular structures exhibit low signal values, and CSF exhibits high signal values. The actual problem lies in the fact that, despite these distinct signal differences between CSF and vessels (nerves), implicit segmentation is not easy, since the signal behavior of the

vessels (nerves) and spinal cord (cranial tissue) hardly differs, while these structures are located in very close proximity to each other. Small vascular or neuronal structures (cranial nerves) can therefore not be sufficiently delineated, and hence segmented, using image tables which only take into account the overall volume. Our strategy was therefore to first isolate CSF and vessels or cranial nerves, and then locally define the transfer function. This approach saves a lot more time and is less susceptible to error than explicit segmentation. The following operations were performed, wherein CSF, vessels and cranial nerves were defined as the foreground, while the spinal cord, cranial tissue and remaining surrounding structures were defined as the background:

1. In most instances, noise suppression is necessary as a first step in order to prepare the data for subsequent post-processing. Highly homogeneous areas are generated using the image processing algorithm of the anisotropic diffusion operator, which yields a better delineation of the object boundaries [11].

2. Before the areas containing CSF and vascular structures can be segmented, an "operation" (closing) oriented to the central gray scale range must be performed, whereby a spherical filter core (kernel) is applied to the voxel data. In this way, both the subarachnoid space and the vasomotor structures are extracted in the form of set geometrical structures (rectangles or squares) in a simple, threshold-oriented operation. The size of the spherical filter core must be larger than the maximum vascular diameter, but smaller than the diameter of the spinal cord or brain stem under examination.

3. After this sorting of data, a narrow gray scale range with a distinctly lower dispersion can be defined. The CSF space can then be segmented by volume growing. "Volume growing" denotes voxel accumulation around a central gray scale range up to a boundary surface. The process of volume growing is executed incrementally so as to be able to tailor the contours as closely as possible to the CSF volume to be extracted.

4. After the CSF volume has been segmented by the preceding operations, supplemental volume growing of the spinal cord or brain stem must also be performed to achieve an exact allocation of overall data to the anatomy.

5. Based on the segmentation results, CSF, spinal cord, brain stem and low-signal surrounding structures can be allocated labeling numbers (*"Tags"*), as shown in Fig. 2. The individual segmentation steps described above thus enable a robust and rapid sorting of data (segmentation).

*Transfer Functions*

After the segmentation steps described in the preceding chapter have been performed, it is possible to use automatic rendering for set transfer functions. A separate function was available for each respectively tagged

sub-volume. These functions reflected correlations between the original data and the used color components and opacities. The user had a total of four different curves available for this purpose. As an example, Fig. 3 shows the transfer functions which led to the rendering in Fig. 5. Another source of information wer the intensity histograms of the volume data records, which is also shown in the diagram of transfer functions (Fig. 3). The opacity was set to constantly low values for the background area ("*Tag 0*"), while a linear threshold was defined for the color components. This resulted in a semi-transparent representation, which facilitated the anatomical orientation. To enable the representation of small vascular structures inside the CSF volume, the opacity was defined in such a way as to yield a threshold-oriented (implicit) rendering ("*Tag 2*"). Starting at a higher opacity for the lower gray scale values of the vascular structures, the threshold valuehad to be adjusted in such a way as to be able to represent CSF as a high intensity transparent area. Darker red for higher intensities enhanced the impression of spatial depth. Green and blue were completely switched off ("*Tag 2*"). The transfer functions for the spinal cord and brain stem ("*Tag 1*") were set to full opacity, wherein green enhances the contrast. To accelerate the process, use was made of predefined tables adjusted to the transfer functions, comparable to those depicted in Fig. 3.

**Results and Discussion**

A total of 20 subjects (10 spinal and 10 brain stem examinations) along with 12 patients with spinal dAV were each examined in the manner described using 3D-CISS sequences, and post-processed using the technique described in "Material and Methods" via direct volume rendering. The examinations were performed on a 1.5 T whole-body MRI system (MAGNETOM Vision, Siemens AG, Medical Solutions). The volumes were comprised of about 40-70 images in all subjects and patients (brain stem 70 images). The matrix measured 512 x 512 pixels. The voxel dimensions were 0.5 x 0.5 x 0.5 mm$^3$. Post-processing took place on a Silicon Graphics Onyx2 (R 10000, 195 MHz) with Base Reality Graphics hardware and a 65 MB texture memory.

Our study clearly shows that only direct volume rendering can ensure sufficiently high-resolution 3D representations of both dAV and vasomotor structures in the brain stem. The following clinical examples are intended to illustrate this.

Fig. 4 demonstrates a complex vascular malformation of the spinal canal in the area of the thoracic spine. Induced by epidural fatty tissue, the "closing" process results in segmentation artifacts, which are partially depicted in Fig. 4 b (red arrows) using the 3D-CISS data record and show low signal irregular structures without allocation to vascular structures. However, choosing the appropriate flexible clip planes makes it possible to eliminate the artifacts easily.
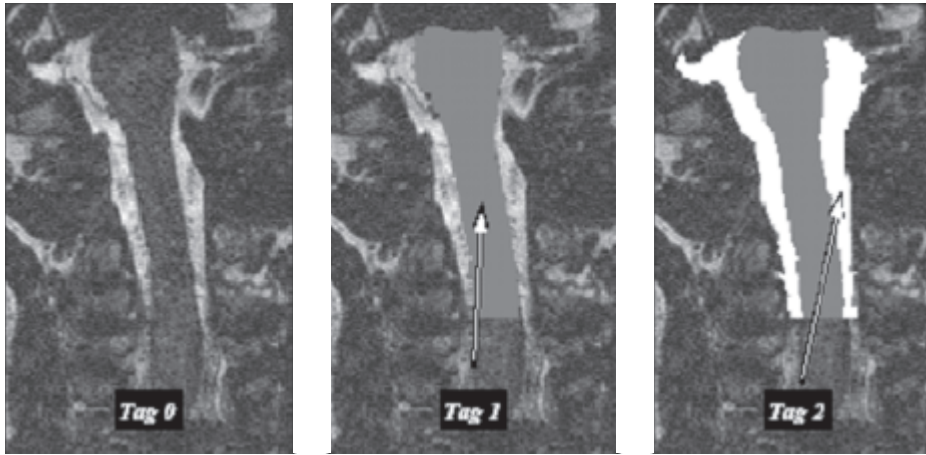
Fig. 2
Sorting of data (segmentation) of a 3D-CISS data record with allocated labeling numbers (*"Tags"*).

Marking of relevant areas: Background (*"Tag 0"*), spinal cord (*"Tag 1"*), CSF and vessels (*"Tag 2"*).
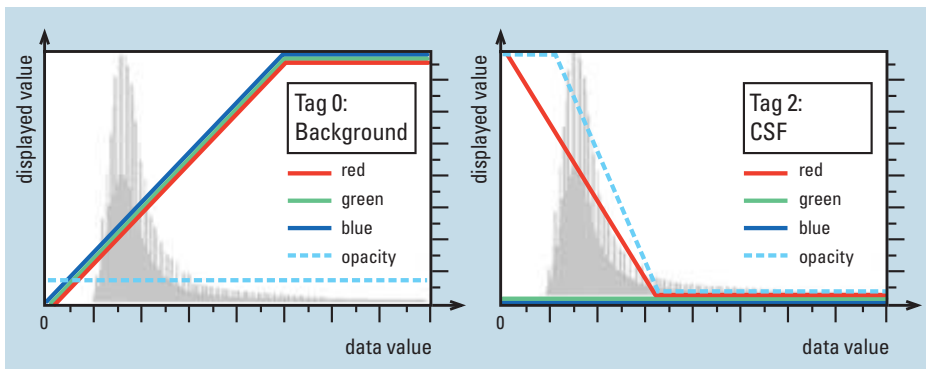


Fig. 3
Transfer functions of varying *"Tags"* as basis for rendering.

Intensity histogram and transfer functions. Settings that lead to the rendering of the 3D data in Fig. 5 (c, d):

(*left*) Arrangement for the semi-transparent background;

(*right*) Arrangement for representing the vascular structures in the CSF volume.
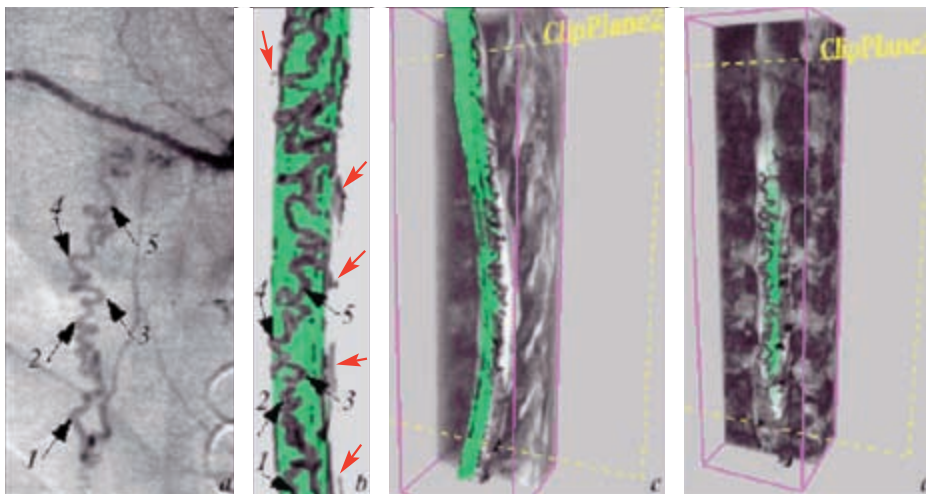


Fig. 4
Improved rendering of a 3D-CISS data record for dAV using the appropriate clip planes in comparison to DSA.

Dura AV fistula of the thoracic spine: Comparison of complex vascular structures (arrows 1-5):

(a) DSA
(b) 3D rendering of a 3D-CISS data record (artifacts: Red arrows)
(c) side view
(d) dorsal (rear) view.

Using the example of a spinal dAV, Fig. 5 shows the spinal vasculature using the invasive technique of DSA, and the noninvasive method of 3D rendering based on the 3D-CISS data record. This example documents the outstanding correlation between a complicated, invasive method not without risk to the patient on the one hand, and the noninvasive MR technique on the other. The spinal canal appears green and highly opaque in the representation, which distinctly improves the spatial allocation. Additional clip planes improve the anatomical orientation via the integration of surrounding structures.

Figs. 6-10 show the results of rendering in the area of the brain stem.

Fig. 6 demonstrates the complete result of rendering a 3D-CISS data record. The brain stem appears green, the arteries are red and the cranial nerves are depicted in yellow. The observer has a frontal view of the vascular and neural structures. The cranial nerves (II-XII) and vascular structures are imaged.

Figs. 7 and 8 show a compilation of rendering results in the respective upper image halves, and the corresponding multi-planar 2D-reconstructions in the lower image halves. Fig. 7 demonstrates the upper brain stem, Fig. 8 the lower brain stem.

Fig. 9 shows that arteries and veins can also be differentiated given a suitable definition of partial volumes. The brain stem and cranial nerves are coded in the same color (yellow). Arteries appear red, and veins blue.

In Fig. 10, a gray-transparent overall data record is superposed over the partial volumes for cranial nerves (yellow), vessels (red) and brain stem (green) as a fourth volume for better orientation. In doing so, the clip plane can be selected to enable the direct spatial allocation of relevant areas. This exemplary image very effectively demonstrates the spatial relationship between the trigeminal nerve (N. V) and the mesiotemporal region, which is characterized by the temporal horns.
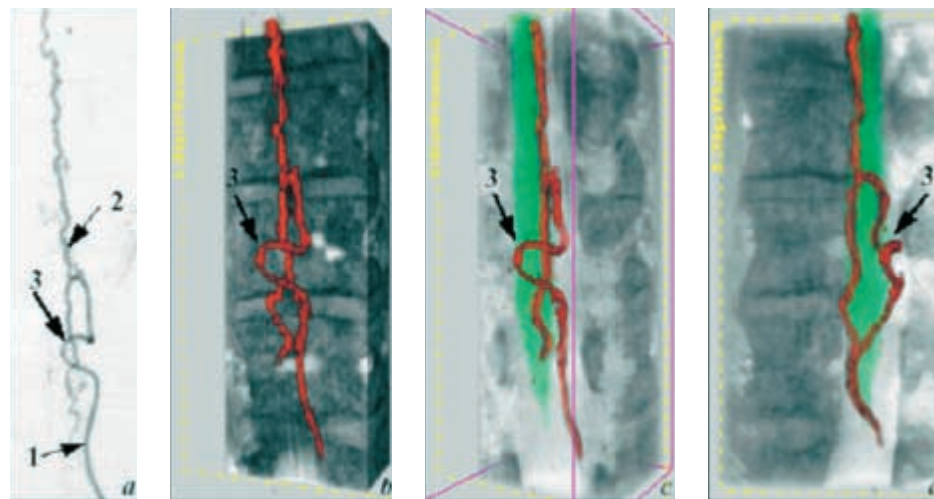


Fig. 5
Comparison of dAV using DSA and 3D-CISS using the direct volume rendering technique.

Dural AV fistula in the area of the lower thoraric spine:

(a) DSA shows the feeder (1) and a perimedullary fistula (2 and 3) –
(b) Direct volume rendering of the MR-CISS data record reveals a good correlation with DSA –
(c, d) Incorporating the surrounding anatomy shows the relationship to the spinal canal and bone structures.
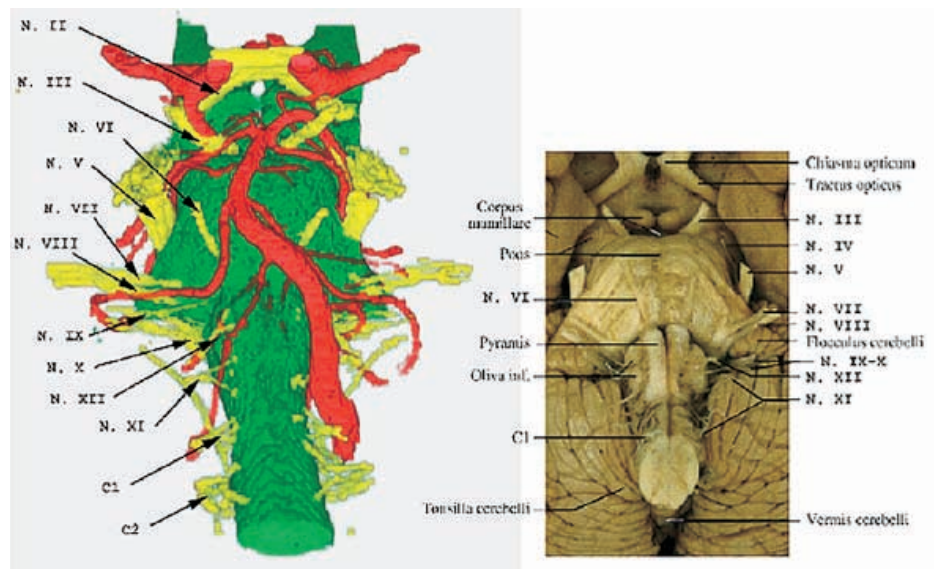
The spinal cord is depicted in green.



Fig. 6
Comparison of 3D-CISS data record rendering of the brain stem using an anatomical preparation.

3D-CISS data record in comparison with an anatomical preparation.
The brain stem appears green, the arteries are red and the cranial nerves are depicted in yellow.

The observer has a frontal view of the vascular and neural structures. The cranial nerves (II - XII) and vascular structures are represented.
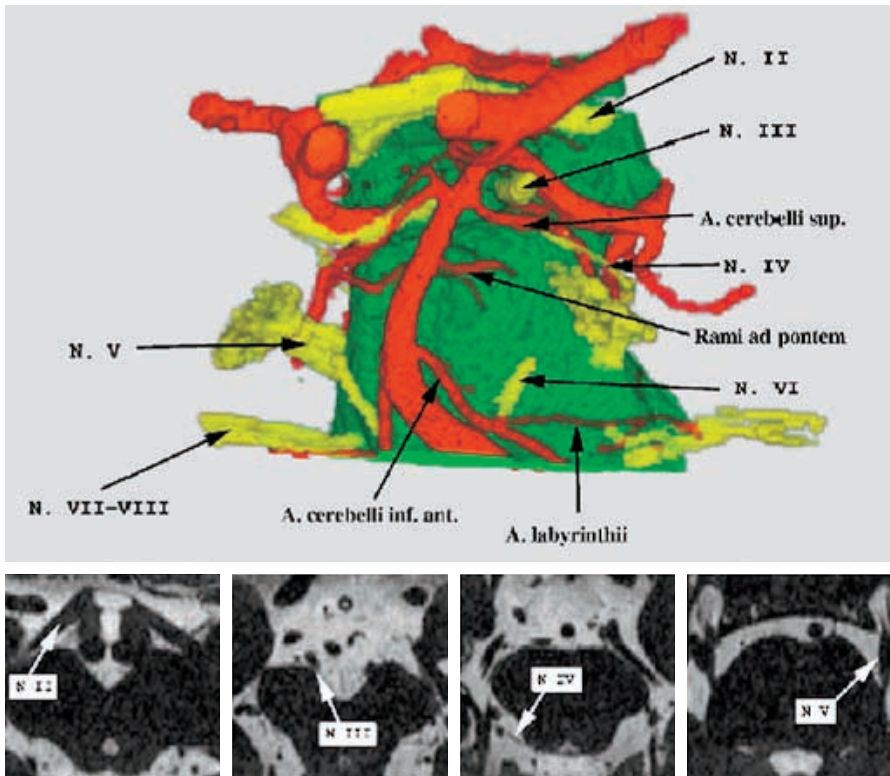
Fig. 7
Results of 3D rendering of the upper brain stem compared to the secondary multi-planar 2D reconstructions.

Compilation of rendering results for a 3D-CISS data record.

The upper brain stem is represented as a 3D image in the upper image half, while the corresponding multi-planar 2D reconstructions are represented in the lower image half.
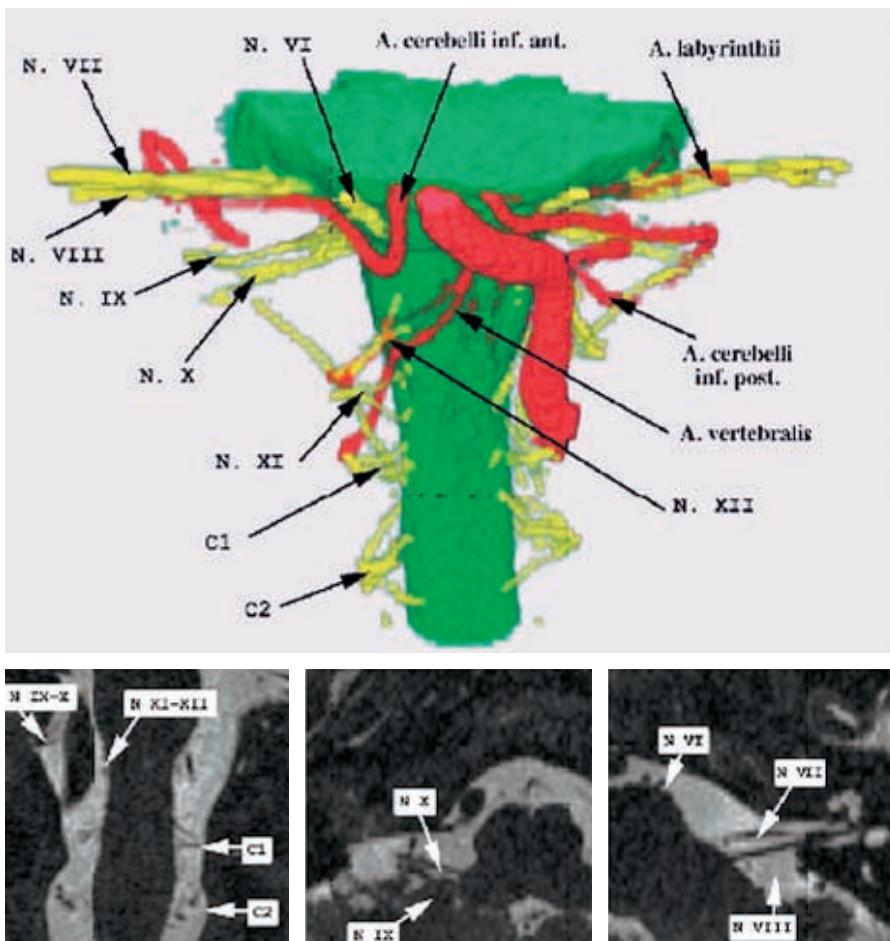


Fig. 8
Results 3D rendering of the lower brain stem compared to the secondary multi-planar 2D reconstructions.

Compilation of rendering results for a 3D-CISS data record.

The lower brain stem is represented as a 3D image in the upper image half, while the corresponding multi-planar 2D reconstructions are represented in the lower image half.

Our results for patients with dura AV-fistula reveal that the spinal vascular structures can be reliably detected with a noninvasive technique, and this detection enables precise planning of the complicated DSA procedure, and hence a significant time savings for the examiner. Opposed to MRI, only the DSA presently offers the resolution necessary to diagnose fistulae, which ultimately indicates the premature transition of the contrast solution from the afferent vessel (arterial) to the efferent vessel [12]. In the future, inclusion of functional aspects (bolus time dynamic plus analysis of flow curves can compensate for this disadvantage using MRI. In the area of the brain stem, due to the good spatial allocation, compression effects of arteries on adjacent cranial nerves might achieve clinical importance in the future.

The dimensions of the target structures and spatial distribution of signal intensities would necessitate a complicated and time-consuming process with respect to 3D-CISS data records given explicit segmentation. The method we developed shows that taking an incremental approach to segmentation yields good results. The time required for segmentation is about 15 minutes in our procedure. Another 5 minutes are necessary for adjusting the transfer functions to the individual patient

data within the framework of rendering when using predefined image tables (look-up table). 3D texture mapping with trilinear interpolation offers a high image rate and excellent image quality for interactive rendering.

## Outlook

In the meantime, the use of new segmentation and rendering procedures has enabled the representation of complex anatomical structures in anatomical quality. As a result, invasive techniques can now be planned, so that the time and, above all, risk associated with examinations can be significantly reduced. Further, this makes it possible to represent minute vascular structures in the area of the spinal canal, yielding a broad range of additional scientific applications. At this time, it cannot be predicted whether CISS sequence will allow to recognize discrete vascular changes even before the dAV is clinically manifest. In this case, the CISS sequence might be suited to make an early diagnosis of dAV or could even be used as a screening tool. At present, the future significance of discrete vascular changes leading up to subsequent clinically manifest malformation in terms of early diagnosis or even targeted screening cannot be predicted. In any event, however, the exact representation
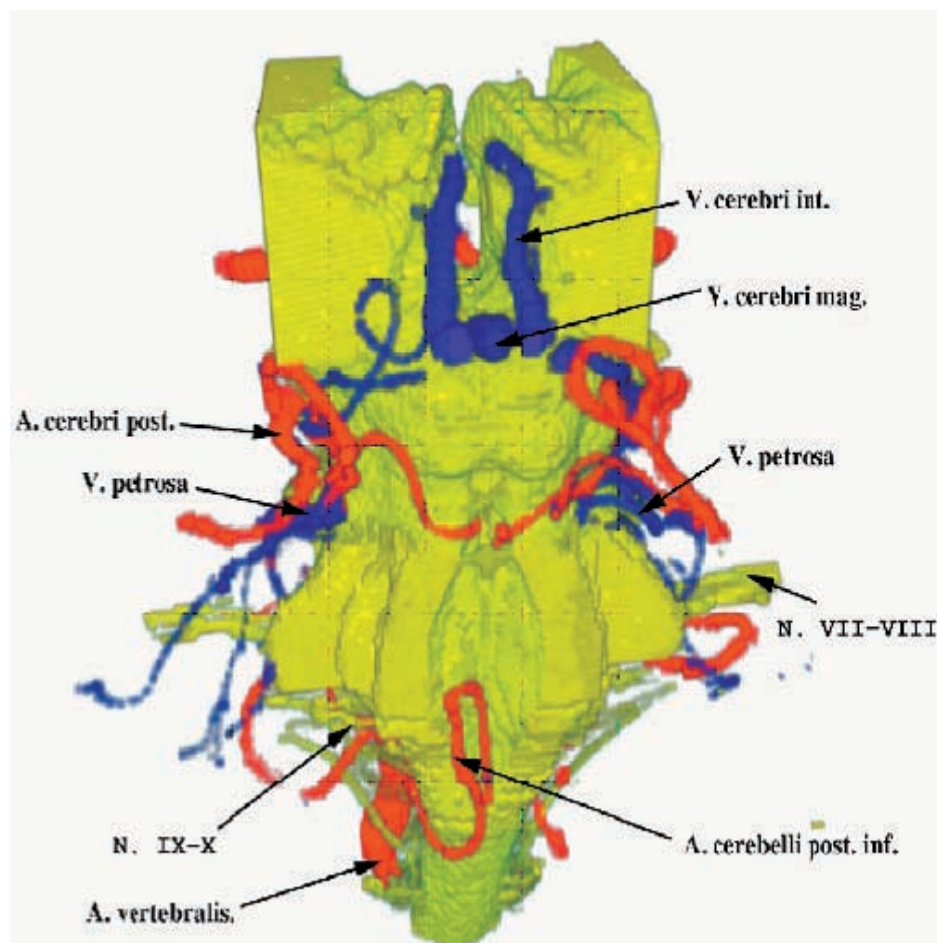


Fig. 9
Rendering of 3D-CISS data record with different indication of arteries and veins using various color codes.

Arteries and veins can also be differentiated given a suitable definition of partial volumes. The brain stem and cranial nerves are coded in the same color (yellow). Arteries appear red, and veins blue.
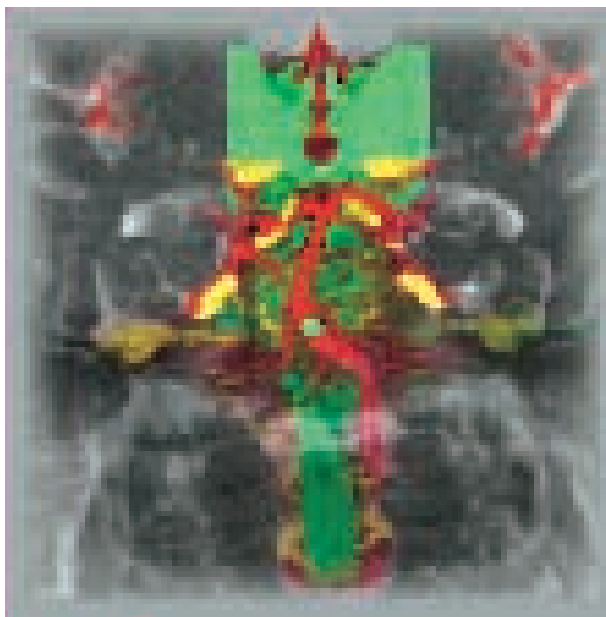
Fig. 10
Rendering of 3D-CISS data record of the brain stem with superimposition of the non-segmented partial residual volume. The temporal horns can be characterized by using the appropriate clip plane.

A gray-transparent overall data record is superposed over the partial volumes for cranial nerves (yellow), vessels (red) and brain stem (green) as a fourth volume for better orientation.

The selected clip plane enables the direct spatial allocation of relevant areas.

This exemplary image very effectively demonstrates the spatial relationship between the trigeminal nerve (N. V, see black arrow) and the mesio-temporal region (see white arrows).

of a defined target volume is the mandatory precondition. In like manner, rendering vasomotor structures in the brain stem opens a series of potential applications (pain symptoms caused by vascular loops, possibly even the triggering of specific forms of hypertension). Other future applications might include navigation-assisted surgery, which can be performed with increasing precision as the ability to accurately represent the target structures improves.

## Abbreviations

| | |
|---|---|
| CISS = | Constructive Interference in Steady State |
| CSF = | Cerebrospinal Fluid |
| CT = | Computed Tomography |
| dAV = | Dura AV-fistulae |
| DSA = | Digital Subtraction Angiography |
| MIP = | Maximum Intensity Projection |
| MRI = | Magnetic Resonance Imaging |
| N. V = | Nervus Trigeminus |
| SSD = | Surface Shaded Display |
| VRT = | Volume Rendering Technique |

Literature

[1] Deimling M, Laub G. Constructive Interference in Steady State for Motion Sensitivity Reduction. Society of Magnetic Resonance in Medicine, Book of Abstracts 1989: 842.

[2] Eberhardt K, Schäfer I, Deimling M, Hollenbach H.-P., Fellner F. Diagnosis of Spinal Dural Arteriovenous Malformations Using a 3D-CISS Sequence. In Proc. of Soc. of Magn. Res. in Med 1997; volume 2.

[3] Nakajima S, Atsumi H, Bhalerao A, Jolesz F, Kikinis R, Yoshimine T, Moriarty T, Stieg P. Computer-assisted Surgical Planning for Cerebrovascular Neurosurgery. Neurosurgery 1997; 41 :403-409.

[4] Melgar M, Zamorano L, Jiang Z, Guthikonda M, Gordon V, Diaz F. Three-Dimensional Magnetic Resonance Angiography in the Planning of Aneurysm Surgery. Comp. Aided Surgery 1997; 2: 11-23.

[5] Kuszyk B, Heath D, Ney D, Bluemke D, Urban B, Chambers T, Fishman E. CT Angiography with Volume Rendering: Imaging Findings. American Jour. of Radiol (AJR) 1995: 445-448.

[6] Rubin G, Beaulieu C, Argiro V, Ringl H, Norbash A, Feller J, Dake M, Jeffrey R, Napel S. Perspective Volume Rendering of CT and MR Images: Applications for Endoscopic Viewing. Radiology 1996; 199 :321-330.

[7] Serra L, Kockro R, Guan C, Hern N, Lee E, Lee Y, Chan C, Nowinsky W. Multimodal Volume-Based Tumor Nerurosurgery Planning in the Virtual Workbench. In Proc. Med. Img. Comput. and Comp.-Assis. Interv. (MICCAI), volume 1496 of Lec. Notes in Comp. Sc. Springer 1998: 1007-1015.

[8] Hastreiter P, Rezk-Salama C, Tomandl B, Eberhardt K, Ertl T. Fast Analysis of Intracranial Aneurysms based on Interactive Direct Volume Rendering and CT-Angiography. In Proc. Med. Img. Comput. and Comp.-Assis. Interv. (MICCAI), volume 1496 of Lec. Notes in Comp. Sc. Springer 1998.

[9] Cabral B, Cam N, Foran J. Accelerated Volume Rendering and Tomographic Reconstruction using Texture Mapping Hardware. ACM Symp. on Vol. Vis. 1994:91-98.

[10] Hastreiter P, Cakmak H. C., Ertl T. Intuitive and Interactive Manipulation of 3D Data Sets by Integrating Texture Mapping Based Volume Rendering into the Open Inventor Class Hierarchy. In Worksh. Bildverarb. f.d. Med. (BVM) 1996: 149-154.

[11] Lacroute P, Levoy M. Fast Volume Rendering Using a Shear-Warp Factorization of the Viewing Transform. Comp. Graphics 1994; 28(4) :451-458.

[12] Hamilton M, Anson J, Spetzler R. The Practice of Neuro-surgery, chapter Spinal Vascular Malformations, Williams & Wilkins 1996: 2272-2292.

Author's address

PD Dr. med. K.E.W. Eberhardt
Institute of Diagnostic and
Interventional Radiology
Municipal Hospital of Schweinfurt
Gustav-Adolf Strasse 8
D-97422 Schweinfurt
Germany

Tel.: +49-(0)9721 720 3209
Fax: +49-(0)9721 720 3333
e-mail: keberhardt@leopoldina.de